Generation of Intermittent Turbulent Events at the Transition from Closed to Open Field Lines in a Toroidal Plasma

T. Happel,[2] F. Greiner,[3] N. Mahdizadeh,[4] B. Nold,[1] M. Ramisch,[1] and U. Stroth[1]
[1]*Institut für Plasmaforschung, Universität Stuttgart, 70569 Stuttgart, Germany*
[2]*Laboratorio Nacional de Fusión, Asociación EURATOM-CIEMAT, Madrid, Spain*
[3]*IEAP, Christian-Albrechts-Universität, 24098 Kiel, Germany*
[4]*ABB Switzerland Ltd. Corporate Research, 5405 Baden-Dättwill, Switzerland*
(Received 19 November 2008; published 23 June 2009)

Turbulent transport at the transition from closed to open field lines has been investigated in the stellarator experiment TJ-K. It is found that drift-wave turbulence in the confined region is responsible for the generation of intermittent structures (so-called blobs) in the unconfined region. There the character of turbulence changes and a decoupling of density and potential fluctuations is observed. The poloidal propagation of the intermittent events can be understood in the framework of background flows caused by gradients in the equilibrium plasma pressure and potential profiles.

DOI: 10.1103/PhysRevLett.102.255001 PACS numbers: 52.25.Fi, 52.25.Xz, 52.35.Ra

Since the early days of turbulence studies in magnetic fusion experiments, the intermittent nature of turbulent transport has been diagnosed and rare but large transport events, named *blobs*, have been identified to carry a significant fraction of the radial energy and particle transport at the plasma edge and in the scrapeoff layer (SOL) [1–4]. Radial transport in the SOL is responsible for the energy load on the first wall and defines the peak power density at the divertor plates of fusion experiments. The relevant radial region is around the natural flow-shear layer at the separatrix which also plays a key role for the improved confinement regime related to the H-mode transport barrier [5]. Hence, the physics of turbulent transport in the vicinity of a flow-shear layer is a key issue for magnetically confined plasmas. But also in space plasmas, intermittent plasma structures are frequently observed as, e.g., in the wakes of planets [6] and satellites [7].

More recent investigations of blobs in fusion devices aim at a better documentation of their statistical properties and of the location where they are generated, as well as at an identification of the instability they are created through [8–10] (for a review, see Ref. [11]). The observation made in the DIII-D tokamak of blobs outside the separatrix and negative density events called *holes* inside [12] points to a blob generation at the separatrix through an interchange type of mechanism. This is supported by fluid simulations [13,14]. Blobs are also observed in linear devices without magnetic-field curvature as, e.g., in the limiter shadow of Q machines [15]. In the magnetized plasma of the LAPD device, zones with holes inside the plasma column and blobs in the limiter shadow can be distinguished [16] and a link between the fluctuations inside and outside the plasma column was found [17]. In the linear VINETA experiment the blobs emerge out of quasicoherent drift waves [18]. In the TORPEX device with a toroidal plasma but open field lines, interchange drive is dominant and blobs originate from an interchange wave [19] and are subsequently powered by the background $E \times B$ flow [20]. For toroidally confined plasmas, however, the instability responsible for blob generation as well as the exact spatial location of their birth have not been identified yet unambiguously.

The present Letter studies blob generation on a microscopic basis. Experiments were carried out in the toroidally confined low-temperature plasma of the stellarator experiment TJ-K. It is shown how blobs are generated at the separatrix by drift-wave turbulence. While *turbulence* refers to broadband fluctuations, *blobs* represent quasicoherent structures. The emergence of blobs in the SOL is studied with high spatial and temporal resolution in a 2-dimensional plane ranging from the plasma edge into the SOL. Ion-saturation current and floating-potential fluctuations were simultaneously measured by Langmuir probes. For the TJ-K plasma it was shown [21] that floating-potential fluctuations can be taken as a measure of plasma potential fluctuations. Because of the low temperature the evolution of turbulent structures and the accompanying $E \times B$ flows can be measured in much greater detail than possible in a fusion plasma. Nevertheless, due to the dimensional similarity of the TJ-K plasma with fusion edge plasmas [22], the results are relevant for fusion experiments.

The low-temperature plasma in the TJ-K stellarator is generated by microwaves at a frequency of 2.45 GHz. It has typical ion and electron temperatures of $T_i \leq 1$ eV and $T_e \approx 7$ eV, respectively, and densities of the order of $n = 5 \times 10^{17}$ m^{-3}. The magnetic field strength of 88 mT corresponds to the electron-cyclotron resonance of the microwaves. Extensive studies of the core plasma and comparisons with simulations from the turbulence code DALF3 [23] have shown that the fluctuations are due to drift-Alfvén-wave turbulence. Observed signatures are that

density and potential fluctuations are almost in phase [22] and that the magnetic component of the fluctuations is small [24]. As expected for drift-wave turbulence the density structures are tilted with respect to the field lines leading to a finite parallel structure length of about 15 m and a perpendicular one of only about 7 cm [25].

For the investigation of the transition from closed to open field lines, the experiment has been modified by introducing a massive toroidal limiter disk which was adjusted to an inner magnetic flux surface. It reduces the area of closed flux surfaces such that the effective minor plasma radius is reduced from $r_{\mathrm{eff}} \approx 10$ to 5 cm and it creates a homogeneous scrapeoff layer between the new separatrix and the one when the limiter is removed (indicated by dashed lines in Figs. 3 and 4). In the homogeneous SOL all field lines have the same connection length of one toroidal turn or about 2 m. At larger effective radii of $r_{\mathrm{eff}} > 10$ cm, the scrapeoff layer is inhomogeneous which means that the connection length varies from one field line to another. This region will be excluded from the analyses.

The Langmuir probes are introduced from the low-field side in the poloidal plane (right side in Fig. 3) which is separated by one field period (60°) from the limiter. A mobile probe with three poloidally aligned tips, two floating and the central one for ion-saturation-current measurements, is used to scan the entire plasma cross section. For correlation analyses, a reference probe is installed in the vicinity of the separatrix in the poloidal measuring plane of the mobile probe (indicated as R_1 in the figures).

The discharges presented in this Letter were in helium at a neutral gas pressure of 3×10^{-4} mbar and a microwave power of 1 kW at 2.45 GHz. The microwave power was injected at −120° and 180° from the limiter and measuring plane, respectively. More details on TJ-K can be found in Ref. [26]. Figure 1 summarizes measurements of the background equilibrium profiles. The density profile (a) was obtained from the ion-saturation current measured with the mobile Langmuir probe and calibrated by a microwave interferometer. The difference between plasma potential and floating potential was used to estimate the electron temperature (a) and an emissive probe was installed for the measurement of the plasma potential (b). From the profiles the plasma background flows u_D were calculated (c). Figure 1(c) shows inferred electron-diamagnetic (circles) and $E \times B$ drift velocities (diamonds). In the plasma center, where the pressure gradient is small, diamagnetic and $E \times B$ drifts cancel. The region with a significant density gradient extends from about $r_{\mathrm{eff}} = 3$ cm across the separatrix throughout the SOL causing a diamagnetic drift of the order of −5 km/s (downward). In this region, the diamagnetic drift dominates the $E \times B$ drift, which reaches a maximum value of about 2 km/s at the separatrix.

The dynamics of the turbulence in the core is found to be similar to the case without limiter, i.e., no distinct mode is present in the power spectrum which exhibits a power law

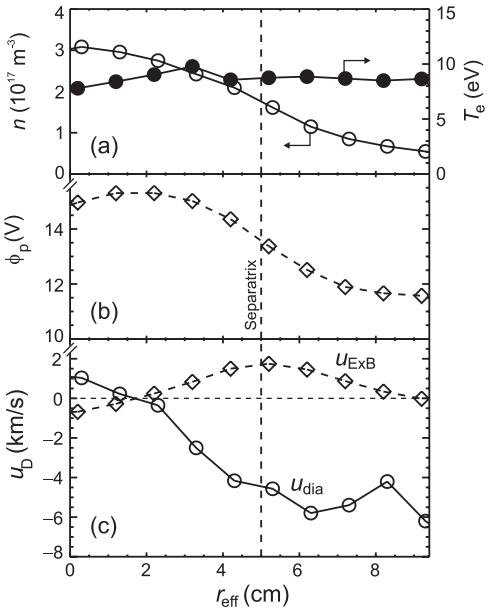

FIG. 1. Radial density [(a), open circles], electron temperature [(a), solid circles], and plasma potential (b) profiles. (c) depicts the inferred diamagnetic (circles) and $E \times B$ drift velocities (diamonds). The vertical line marks the separatrix position. Positive drift velocities point upward into the z direction.

behavior from 10 to 100 kHz with a spectral index of ≈3.5. The measured autocorrelation time is about 60 μs and the PDF is negatively skewed ($S \approx 0.8$). In order to get further information on the character of the turbulence, the poloidal propagation velocity v_θ of turbulent fluctuations was deduced from a cross-correlation analysis of two poloidally separated probes measuring the ion saturation current. From the time delay in the correlation function and the probe distance, the poloidal propagation velocity v_θ is calculated. Figure 2 depicts the resulting radial profile $v_\theta(r_{\mathrm{eff}})$. In the confined plasma, the fluctuations propagate with a velocity of 1–2 km/s into the electron-diamagnetic drift direction. This has to be compared with the drifts presented in Fig. 1. As shown later (Fig. 3), the radial correlation length of the structures in the confined plasma is $L_{\mathrm{corr}} \approx 3$ cm. For the comparison, the drift velocities from Fig. 1 are radially averaged over this region and then amount to $\bar{u}_{\mathrm{dia}} \approx -2.5$ km/s and $\bar{u}_{E\times B} \approx 1$ km/s. Hence, the measured propagation velocity of the turbulent structures in the confined plasma is consistent with drift waves which propagate with the sum of diamagnetic and $E \times B$ drift velocities $v_\theta \approx \bar{u}_{\mathrm{dia}} + \bar{u}_{E\times B} \approx -1.5$ km/s. This is one indication that the limited plasma in the confinement region behaves the same as the confined plasma without limiter. Furthermore, the cross phase between density and potential fluctuations remains small in the reduced plasma cross section.

In the vicinity of the separatrix, the propagation direction of the fluctuations switches to the direction of the ion-diamagnetic drift. This is in variance with drift-wave tur-

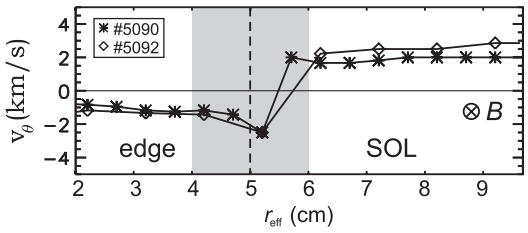

FIG. 2. Poloidal velocities of density fluctuations from correlation analyses between two Langmuir probes. The shaded area indicates the uncertainty in the separatrix position.

bulence. The observed velocity of $v_\theta \approx +2$ km/s is in reasonable agreement with the average $E \times B$ drift velocity of $\bar{v}_{E\times B} \approx +1$ km/s. The change of the propagation velocity in the plasma rest frame indicates a change in the character of turbulence. An obvious reason for this change could be that the parallel drift-wave dynamics, which needs the measured parallel wavelengths of about 15 m to develop, is suppressed due to the reduced connection length of 2 m in the scrapeoff layer.

In order to investigate the generation of turbulent structures (blobs) in the scrapeoff layer of TJ-K, conditional averaging (CA) [27] was applied to data from the moving Langmuir probe system and the reference probe. Time series of 10^6 points were sampled at 1 MHz with both fixed and moving probes simultaneously. A rectangular box of 23 × 18 cm^2 was scanned with a spatial resolution of 1 cm. The experiment was done with the reference probe measuring floating potential while the two tips of the moving probes measured ion-saturation current and floating potential. Thus the CA analysis reveals the spatiotemporal evolution of turbulent density and potential structures. The entire data set was taken in a single discharge of 30 min duration.

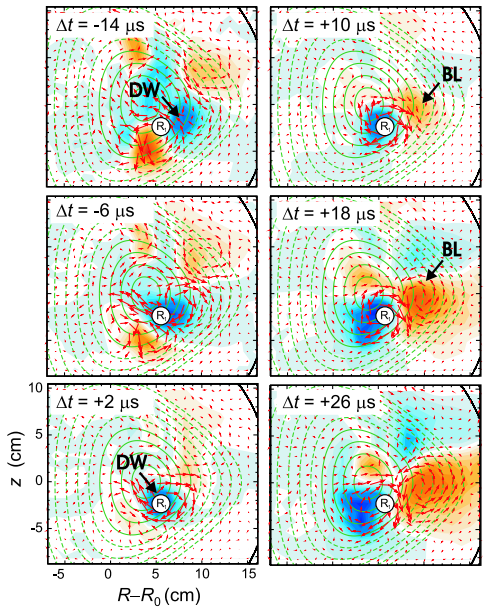

FIG. 3 (color online). Evolution of potential structures from conditional averaging at different time lags Δt. The $E \times B$ drift as calculated from the potential structures is indicated by arrows. Flux surfaces with closed and open field lines are plotted as continuous and broken lines, respectively. The reference probe was at R_1 as indicated and the condition was set to a negative value of the floating potential of 2σ. Blue (DW) corresponds to negative density values and orange (BL) to positive ones.

The result of the CA procedure can be presented as a movie where each picture consists of a 2-dimensional plot of the conditional average at a specific time lag Δt between the data from the reference and the moving probes. The 2-dimensional data can be interpreted as a characteristic turbulent structure. By varying the time lag Δt, the temporal evolution of the structure is visualized.

Figure 3 depicts the CA results for six different values of the time lag ($\Delta t = -14$ to $+26$ μs). The condition was set to rising negative values of twice the rms value of the floating-potential fluctuations. Blue areas (DW) indicate negative density fluctuation amplitudes and orange (BL) stands for positive ones. To get insight into the dynamics on all scales, in each picture the maximum amplitude is scaled to 1. In addition to the density structures, the $E \times B$ drift as calculated from the potential structures measured simultaneously is indicated by arrows. The magnetic flux surfaces are plotted by continuous or broken lines when the field lines are closed or open, respectively. The fact that structures can be seen in the confinement region as well as in the SOL shows that fluctuations outside and inside the separatrix are closely correlated.

Following the trajectory of the blue structure (DW →) in the region of closed field lines, one recovers the propagation into the electron-diamagnetic direction of the drift wave. Around zero time lag ($\Delta t = +2$ μs), the negative density structure is centered around the reference probe. Since the reference probe measures floating potential this shows an important property of drift-wave turbulence, namely, that density and potential fluctuations are in phase.

The generation of a positive density structure (blob BL →) in the scrapeoff layer can be traced from $\Delta t = +18$ μs on. The blob barely moves while the $E \times B$ vortex of the drift wave continues to feed it with density from the core. This continuous growth of the blob can be attributed to the difference in poloidal propagation velocity of the fluctuations inside and outside the separatrix, as documented in Fig. 2. The drift wave continues to propagate into the electron-diamagnetic drift direction while the structure outside is immobile for about 10 μs. Hence the outward particle flow associated with the vortex related to the drift-wave structure can continuously feed the blob. This is different from the observations made in Ref. [20], where an interchange wave creates the blobs across a shear layer. At this point it is appropriate to comment on the shear layer at the separatrix visible in Fig. 2. A shear layer close to the separatrix has been observed in other devices,

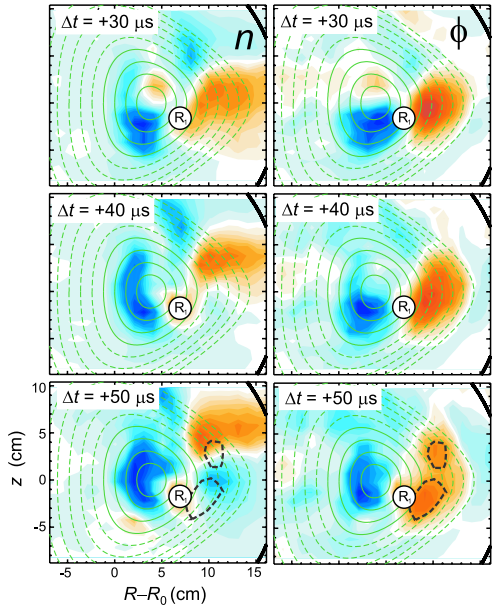

FIG. 4 (color online). Evolution of density (left) and potential (right) fluctuations for $\Delta t > 30$ μs. The decoupling of density and potential structures takes place in the SOL region and is gradual. In contrast, in the core region density and potential structures are still coupled. To guide the reader, in both lower plots a potential contour is shown (dashed line).

too [28–30]. It is usually attributed to a rapid change of the radial electric field on the transition from closed to open field lines. Other than in high-temperature plasmas, in TJ-K the radial electric field is small ($\approx$60 V/m in Fig. 1). The shear layer seen in the poloidal velocity of the fluctuations emerges from a change in the turbulence characteristic due to the limited connection length in the SOL. This shows that depending on the magnetic configuration, there might be different paths to blob generation in the SOL of fusion plasmas.

Figure 4 illustrates the further evolution of the blob. Here both density (left column) and potential structures (right column) are depicted for larger time lags. Focusing on the SOL region, the previously created blob (cf. Fig. 3) starts to move mainly due to the background $E \times B$ flow. Because of direct contact of the field lines with the limiter, the parallel drift-wave dynamics is suppressed. Consequently, for $\Delta t > 30$ μs a gradual decoupling of density and potential structures in the SOL becomes apparent. That density and potential structures get out of phase can be seen at $\Delta t = 50$ μs from the overlayed dashed lines which highlight a positive potential contour. This shows that turbulence in the SOL is clearly not drift-wave–like. In contrast, density and potential structures in the confinement region remain in phase.

In summary, for the first time the generation of intermittent density fluctuations has been studied on a microscopic level and with high spatial and temporal resolution at the transition from closed to open magnetic-field lines of a toroidally confined plasma. For the investigated low-temperature plasma it could be shown that blobs in the scrapeoff layer are generated by drift-wave turbulence from the confinement region. As a key element in the process, the change of the turbulent characteristics at the separatrix has been identified. This transition occurs due to the breakdown of the parallel drift-wave dynamics on the open field lines and a resulting shift of the phase between density and potential fluctuations away from the drift-wave value of zero. This finding is of major importance for the understanding of turbulent transport in the scrapeoff layer of fusion plasmas.

[1] S. J. Zweben, Phys. Fluids **28**, 974 (1985).
[2] M. Endler *et al.*, Nucl. Fusion **35**, 1307 (1995).
[3] R. A. Moyer *et al.*, Plasma Phys. Controlled Fusion **38**, 1273 (1996).
[4] E. Sánchez *et al.*, Phys. Plasmas **7**, 1408 (2000).
[5] P. W. Terry, Rev. Mod. Phys. **72**, 109 (2000).
[6] D. A. Gurnett, *et al.*, J. Geophys. Res. **87**, 1395 (1982).
[7] C. L. Henderson *et al.*, Planet. Space Sci. **15**, 1499 (1967).
[8] G. Y. Antar, G. Counsell, Y. Yang, and P. Devynck, Phys. Plasmas **10**, 419 (2003).
[9] J. A. Alonso *et al.*, Plasma Phys. Controlled Fusion **48**, B465 (2006).
[10] M. Agostini *et al.*, Phys. Plasmas **14**, 102305 (2007).
[11] S. J. Zweben *et al.*, Plasma Phys. Controlled Fusion **49**, S1 (2007).
[12] J. A. Boedo *et al.*, Phys. Plasmas **10**, 1670 (2003).
[13] D. A. Russell *et al.*, Phys. Rev. Lett. **93**, 265001 (2004).
[14] W. Fundamenski *et al.*, Nucl. Fusion **47**, 417 (2007).
[15] D. P. Sheehan *et al.*, Phys. Plasmas **4**, 3177 (1997).
[16] T. A. Carter, Phys. Plasmas **13**, 010701 (2006).
[17] G. Y. Antar, J. H. Yu, and G. Tynan, Phys. Plasmas **14**, 022301 (2007).
[18] T. Windisch, O. Grulke, and T. Klinger, Phys. Plasmas **13**, 122303 (2006).
[19] I. Furno *et al.*, Phys. Plasmas **15**, 055903 (2008).
[20] A. Diallo *et al.*, Phys. Rev. Lett. **101**, 115005 (2008).
[21] N. Mahdizadeh *et al.*, Plasma Phys. Controlled Fusion **47**, 569 (2005).
[22] U. Stroth *et al.*, Phys. Plasmas **11**, 2558 (2004).
[23] B. Scott, Plasma Phys. Controlled Fusion **39**, 1635 (1997).
[24] K. Rahbarnia *et al.*, Plasma Phys. Controlled Fusion **50**, 085008 (2008).
[25] N. Mahdizadeh *et al.*, Plasma Phys. Controlled Fusion **49**, 1005 (2007).
[26] N. Krause *et al.*, Rev. Sci. Instrum. **73**, 3474 (2002).
[27] H. Johnsen, H. L. Pécseli, and J. Trulsen, Phys. Fluids **30**, 2239 (1987).
[28] C. P. Ritz *et al.*, Phys. Fluids **27**, 2956 (1984).
[29] C. Hidalgo *et al.*, Plasma Phys. Controlled Fusion **43**, A313 (2001).
[30] J. Bleuel *et al.*, New J. Phys. **4**, 38 (2002).